I&EC research
Industrial & Engineering Chemistry Research

Article

pubs.acs.org/IECR

A Validated Flowsheeting Tool for the Study of an Industrial Granulation Process

Ivana M. Cotabarren,* Diego E. Bertín, Verónica Bucalá, and Juliana Piña

Department of Chemical Engineering, PLAPIQUI, Universidad Nacional del Sur, CONICET. Camino La Carrindanga Km. 7, 8000 Bahía Blanca, Argentina

ABSTRACT: This work evaluates the capabilities of a complete dynamic simulator developed for a urea granulation circuit (based on fluidized bed technology) to analyze the process sensitivity against different disturbances and to study common operating problems. First, the circuit model is validated by comparing simulation results with plant data from a high capacity industry. On the basis of a sensitivity analysis of the process variables, diverse strategies are explored aiming to solve typical operational challenges (i.e., granulation temperatures that are too high, undesired dust formation, low fluidized bed heights, etc.) by considering different control variables or alternative flowsheet configurations. It is demonstrated that an appropriate fluidization air distribution between the different granulator chambers allows control, within certain limits, of the often too-high fluidized bed temperatures. Furthermore, it is shown that by adjusting the total granulator pressure drop, the fluidized bed levels can be kept within the desired ranges. Finally, the developed flowsheeting tool suggests that the partial bypass of the fines generated in the crusher can be an efficient strategy for improving the product on-specification while the circuit variables remain within the desired operating range.

1. INTRODUCTION

It is widely accepted that the development of computing tools for the simulation of large-scale processes has been one of the most important engineering progresses. Nowadays, there is a wide variety of commercial packages that allow not only simulating complete flowsheets but also optimizing and developing control strategies on different processes among other important tasks (e.g., AspenTech,[1] gPROMS,[2] Pro/II[3]).

Even though the number of industries that handle particulate materials is vast, today's commercial flowsheet simulators mainly focus on fluid processes. Consequently, the simulation of integrated solid processes is not as advanced; it is rather common to model, simulate, design, and optimize each unit individually.[4] This is due to the complexity of modeling solid systems. Engineering processes involving fluids require relatively few variables to describe the system behavior completely (e.g., temperature, composition, pressure), whereas when handling solids, the process streams are required to be described by lumped variables as well as by distributed properties (e.g., particle size, porosity, moisture distributions) that require the use of the population balance and several additional parameters to solve the unit models.[4−7]

Within particle technologies, granulation is a fundamental operation of widespread use. It converts fine particles and/or atomizable liquids (suspensions, solutions, or melts) into granular material with the desired properties.[8] In general, this size enlargement process cannot be considered isolated; instead, interactions with other peripheral operations must be taken into account. The combination of all the involved units constitutes the granulation circuits. Traditionally, the design and operation of these circuits were performed under trial and error and on the basis of previous experiences.[9] Lately, together with the progress in numerical techniques and computer resources, great effort has been invested in shifting granulation processes from art to science.[10]

Investigation focusing on process modeling for the development of simulators for the solid industry has been particularly intense. On this subject, a group of German universities developed the software SolidSim, recently acquired by AspenTech.[1] This environment allows steady-state and dynamic simulation of systems that handle streams with distributed properties, such as the particle size distribution.[4,5,11−13] Another example of solid simulators is gSOLIDS, implemented under the gPROMS environment. gSOLIDS also presents a broad library of solids unit operations that can be used, among others purposes, to perform steady-state and dynamic simulations, steady-state and dynamic optimizations, parameter estimation, and process control.[2] Even though nowadays the simulators for solid processing allow representation of a wide variety of unit operations (separation, size reduction, size enlargement, etc.), as it happens for the fluid processes simulation, the provided standard unit models may be not suitable to properly represent the physical behavior of a particular equipment, even after parameter fitting procedures. In those situations, the programming of ad hoc models is required.

Because granular urea is the most-consumed nitrogen-based fertilizer, with a forecasted increase of 44 million tons in plant capacity to reach a total of 226.1 million tons in 2016,[14] the production of this fertilizer is critical in the modern agriculture scenario. For this reason, in this work, the potential improvement in the granular urea process performance is studied by applying flowsheeting tools. In the early stages of the development of a urea flowsheet simulator based on UFT fluidized bed granulation technology,[15] the suitability of using

Received: May 23, 2013
Revised: August 29, 2013
Accepted: September 26, 2013
Published: September 26, 2013

ACS Publications © 2013 American Chemical Society

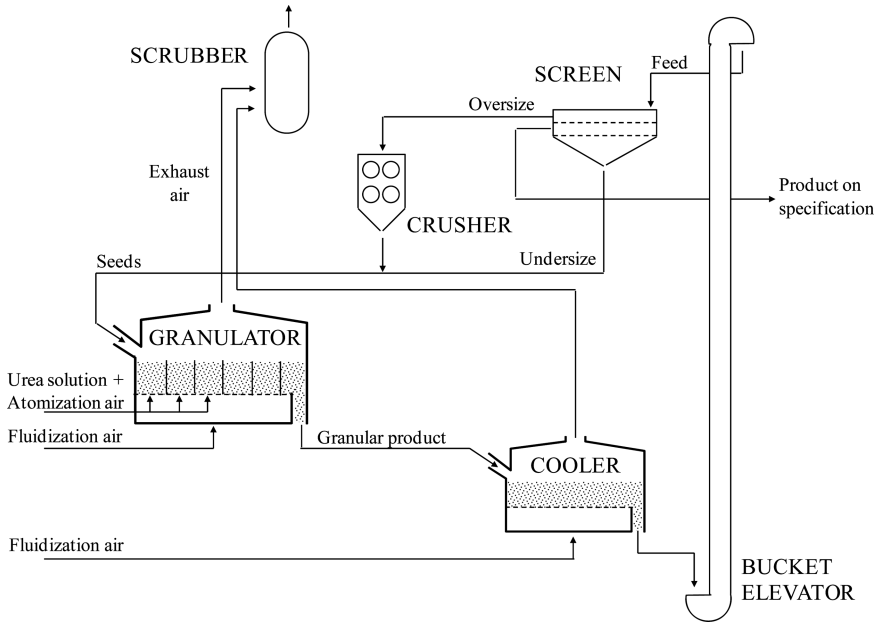

Figure 1. Urea granulation circuit based on UFT fluidized bed granulation technology.[15]

the solids package provided by AspenTech[1] to represent the urea granulation circuit performance was evaluated. Nonetheless, the existing models were not able to properly describe the available data of a high capacity urea plant. According to this, our research group developed the simulator presented in this contribution, with ad hoc models for the units involved in the UFT fluidized bed granulation technology (i.e., multichamber fluidized bed granulator, fluidized bed cooler, double-deck vibrating screens, and double-roll crushers). All the models were developed and integrated in gPROMS environment. In this work, the developed flowsheeting tool is first validated against plant data and then used to explore diverse strategies aiming to solve typical operational challenges.

2. SIMULATION ENVIRONMENT AND MATHEMATICAL MODELS

Among all the different types of size enlargement units, the urea industry prefers the fluidized bed granulators, basically because they couple a number of processes into a single step (i.e., particle growth, wetting, drying/solidification, mixing, cooling).[8,16] Besides the granulator, a typical urea granulation flowsheet based on UFT fluidized bed granulation technology (Figure 1) includes a cooling unit to diminish the granules' temperature and avoid undesirable lump formation, double-deck screens to remove the under and oversize particles from the desired product, and double-roll crushers to grind the oversize material and return it to the granulator as seeds together with the undersize stream.[15,17] The seeds are constantly fed to the fluidized bed granulator while a concentrated urea solution (usually called urea melt due its high urea concentration, which is about 96 wt %[15,18,19]) is sprayed from the bottom of the unit. The particles grow by deposition of the concentrated solution onto their surface and the subsequent evaporation of the water content and solidification of the urea present in the droplets, phenomena promoted by the fluidization air.[20]

Considering the technology studied in this contribution, the granulation unit is constituted by several chambers (six in particular) that operate in a bubbling fluidized regime (Figure 2). The first three compartments are for granules growth and the last three are for particles conditioning and cooling.[18,19] Fluidization air is delivered to the granulator lower casing and distributed by a perforated plate, suspending the urea particles in the upper casing and being exhausted at the granulator top. This air is taken at atmospheric conditions by a single blower and later derived to each chamber by a series of dampers. The air that enters into the growth chambers can be preheated by heat exchangers, which allow regulation of the fluidization air temperature to a certain level.[21,22] The granulator chamber's temperatures are not only determined by the sensible heats corresponding to the streams that enter and/or leave each chamber but also by latent heats associated with the urea solidification and water evaporation. As a result, the granulator's first three chambers normally operate between 109 and 112 °C. Temperatures higher than 100 °C guarantee the solution water evaporation, and temperatures lower than 133 °C avoid undesired agglomerate formation by urea particles' melting.[21,22] The last three chambers operate between 70 and 90 °C because the particles are fluidized with air at ambient conditions, and no urea solution at high temperature is atomized.[22]

Figure 2 also depicts the urea solution injection system. The urea solution is atomized as very fine droplets by means of binary nozzles located just above the perforated plate (bottom sprayers). The atomization air temperature is between 130 and 135 °C in order to avoid solidification of the urea solution and at a pressure between 1.2 and 4 bar to favor the formation of very small droplets of about 20−120 μm.[18,22] In this type of unit, bottom spray is preferred over top spray to minimize the elutriation of droplets that may solidify before reaching the particles' surface. In order to minimize dust formation, the use of a urea solution with a water concentration not higher than 5 wt % (i.e., the use of highly urea concentrated solutions) is also recommended.[21,22]

The chambers are delimited by separating weirs with openings at the bottom that allow the particles' underflow by the principle of communicated vessels.[20] The fluidized bed levels within each chamber have to remain below the height of

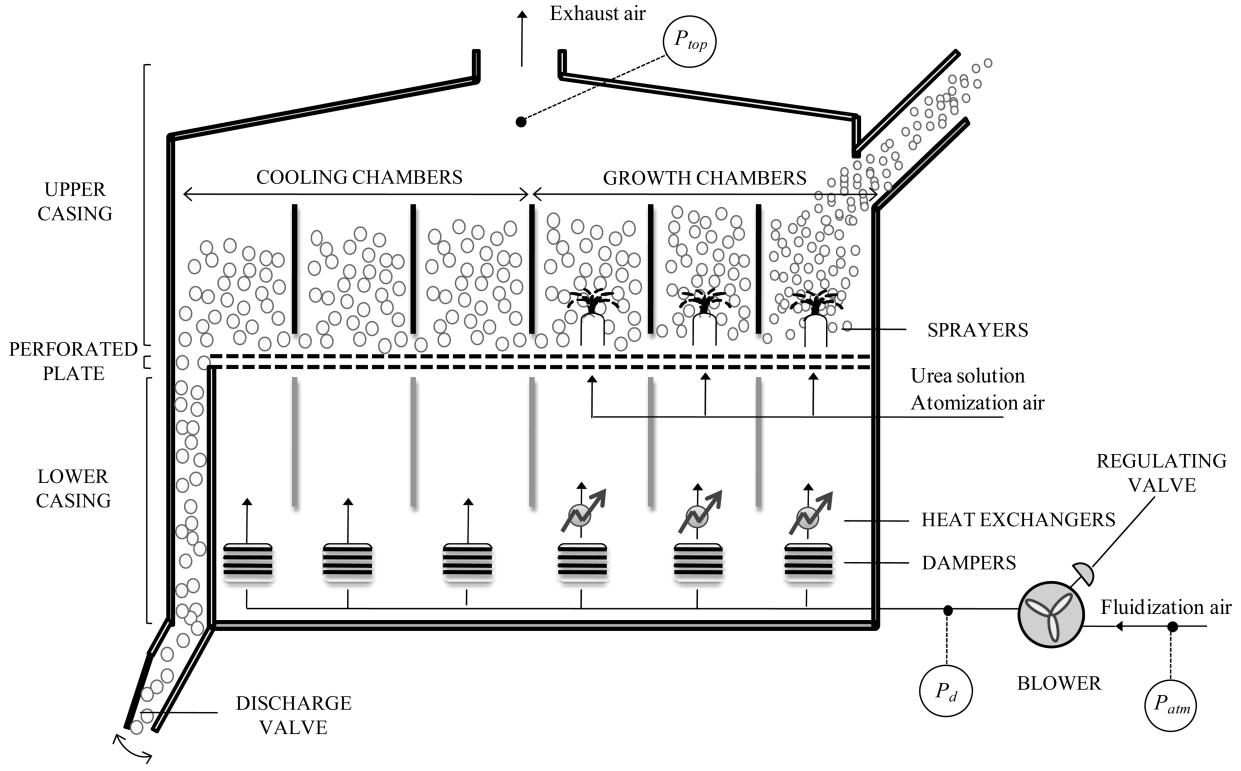

Figure 2. Granulation unit.

the separating weirs to ensure that no solids will overflow and above a minimum recommended height to guarantee that no drops will be sprayed over the fluidized beds in the growth chambers.[21,22] The granulator product discharge is performed by ducts located at the bottom of the last chamber. These ducts present swing-type valves that can be adjusted to regulate the solids discharge.[18,23]

The granulation unit operates at constant total pressure drop by regulation of the fluidization air blower valve position.[16] This total pressure drop is given by the difference between the granulator top pressure (P_{top}, Figure 2) and the atmospheric pressure at the fluidization air blower suction (P_{atm}, Figure 2). To favor dust extraction, the granulator top is maintained under a certain vacuum (usually between −0.004 and −0.0044 bar_{gauge}[18,21]) by means of downstream exhaust fans. The granulator chambers operate as parallel systems, that is, with the same total pressure drop. Therefore, against any change in the chambers' hold-up, the fluidization air is automatically redistributed.

The simulator used in this work includes a fluidized bed granulator model developed in previous contributions.[24,25] This model was based on coating as the main size enlargement mechanism and allows the dynamic mass, energy, momentum, and population balances to be solved for all the granulator chambers. Details of the granulator model's formulation can be found in the Appendix.

After the particles leave the granulation unit, the product stream is fed into a fluidized bed cooler. This unit operates as one of the granulator cooling chambers; therefore, the previous model was adapted for the particular design and operating features of the cooler, when the urea solution injection is assumed equal to zero.

The circuit classification step is performed by double-deck vibrating screens situated downstream from the fluidized bed cooler. The mathematical model that represents the performance of this unit was developed in a previous contribution and validated against industrial data from a high capacity granulation plant.[26]

The particles classified as oversize by the screens are then fed to double-roll crushers with variable gaps (one between the upper pair of rolls and one between the lower pair) in order to reduce their sizes and be suitable to be incorporated into the granulator as seeds. The model developed for this unit was also previously developed and allows prediction of the particle size distribution (PSD) of the fragmented particles as a function of the feed PSD and gap settings. The parameters corresponding to this model were fitted against industrial data, as well.[17]

The urea granulation circuit model, including each unit mathematical representation, was implemented under the gPROMS Model Builder environment. This is a multipurpose tool mainly used to build and validate process models, including steady-state and dynamic optimizations among several other functions.[27] Its flexibility and robustness has been widely proved by many other workers, even for processes involving particulate solids such as antisolvent crystallization.[28]

The complete circuit simulator was first implemented by Cotabarren et al.[29] without considering the granulation unit momentum balance equation (i.e., eq A.8; see the Appendix). Using this simulation tool, steady-state optimizations were performed by manipulating the crusher gap, screens apertures, and melt flow rate.[29] A posteriori, different optimal control studies were carried out in order to maximize the plant throughput.[23]

In this work, an upgraded simulator is used. The improvement is related with the granulator model, which now takes into account the unit momentum balance to evaluate the fluidization air flow rate that is delivered to the granulation device. In the following section, the new flowsheeting tool is first validated

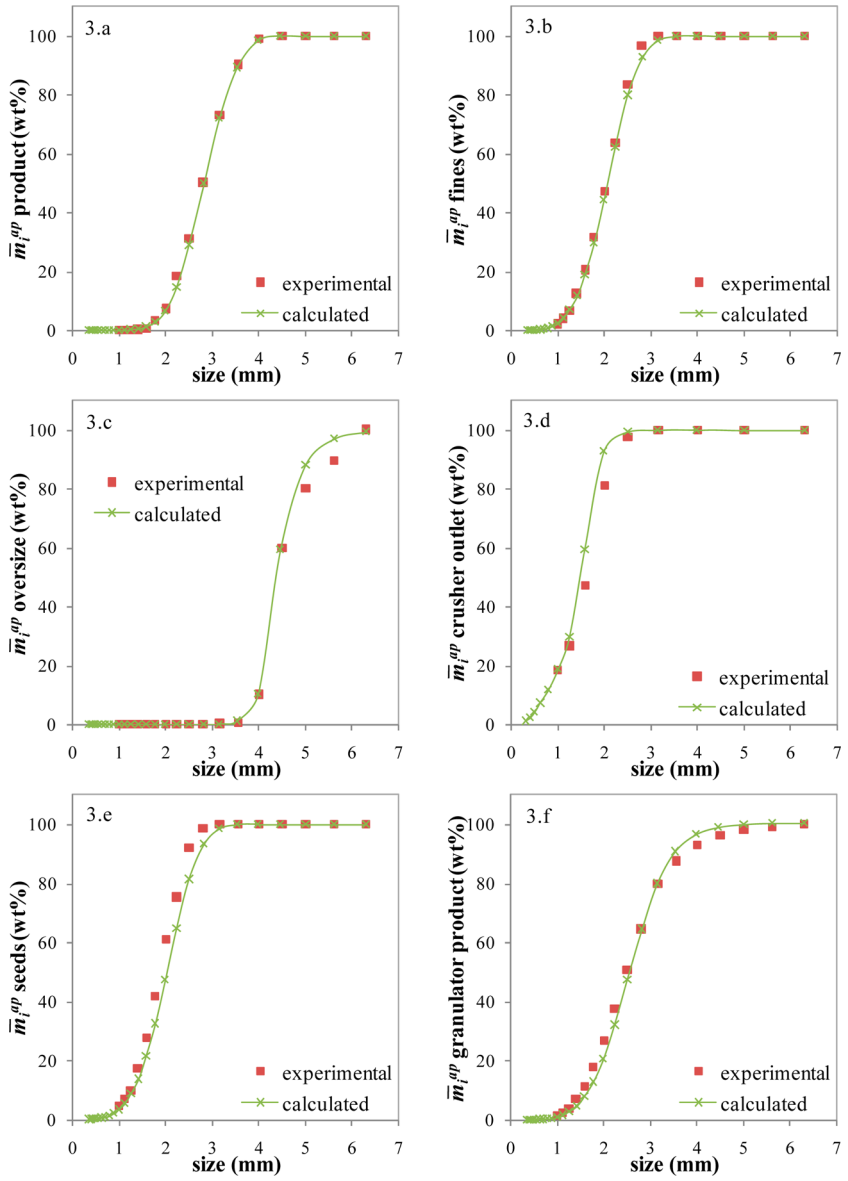

Figure 3. Correspondence between the experimental and simulated PSDs for all the circuit streams at a selected final steady state.

against experimental data. Then, it is used to study common operating problems.

3. RESULTS AND DISCUSSION

3.1. Granulation Circuit Model Validation. In this section, the urea granulation process simulator is validated by comparing the simulation results against industrial data corresponding to a high capacity urea plant. The experimental data were collected during two planned tests that involved only changes in the gaps between the lower (during test 1, from 1.6 to 1.4 mm) and upper (during test 2, from 2.5 to 2.1 mm) pairs of the crusher rolls. All the particle streams were sampled every 4 h for a total period of 36 h during test 1 (i.e., 10 samples). For test 2, the first sample was withdrawn after 18 h, then the particulate samples were collected every 12 h (because this test lasted 78 h, 7 samples were available). Overall, three different steady states were analyzed. The simulator was run under the industrial operating conditions and for the geometric parameters of the plant units.

Figure 3 shows the agreement between the experimental and simulated data for the PSDs of the main streams (expressed as passing cumulative mass fractions) at one of the selected steady states (i.e., last sample of test 1). As it can be seen, there is an excellent correspondence for all of the streams, especially for the product (marketable granules), the fines classified by the screen, and the granulator product (Figure 3a, b, and f). The correlation for the oversize classified by the screen, the granulator seeds, and the crusher outlet is not as good but is still acceptable (Figure 3c, d, and e). The results indicate that the developed model is quite satisfactory to predict the PSDs of the streams when the plant steady state is reached.

Figure 4 presents the correspondence between the experimental and simulated data for the plant product PSDs at the three different steady states and every sampling hour (i.e., the simulated data are calculated by means of the circuit dynamic model). As it can be seen, the simulator predicts the product stream PSD in a very satisfactorily way. Furthermore, from the 289 simulated points (17 sample hours of 17 classes each), 80% are within a 2 wt % deviation with respect to the

dx.doi.org/10.1021/ie401650r | Ind. Eng. Chem. Res. 2013, 52, 15198−15210

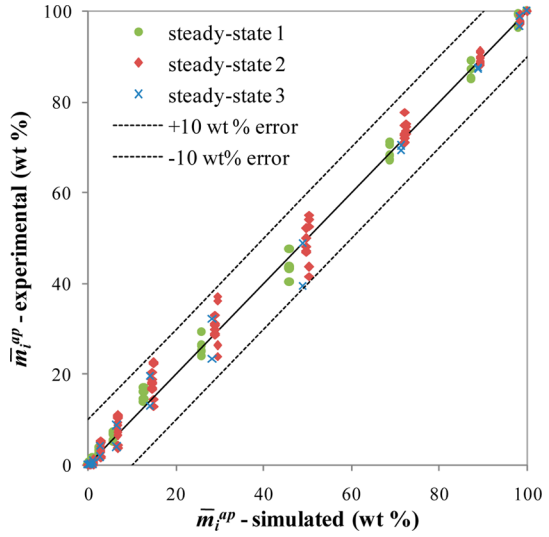

Figure 4. Correspondence between the experimental and simulated PSDs for the product stream at every sampling time.

experimental data; presenting all of them results in deviations smaller than 10 wt %.

One of the most important parameters in the fertilizer industry is the size guide number (SGN), which is the median (i.e., granule size for which the passing accumulative fraction reaches the 50 wt % value) of the mass particle size distribution multiplied by 100. As can be seen in Figure 5, the prediction of

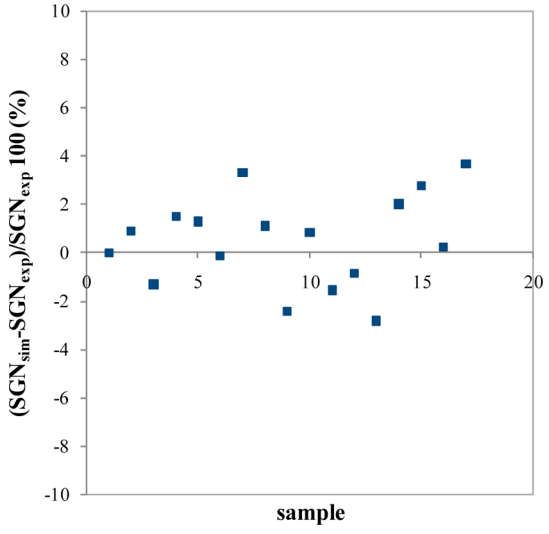

Figure 5. Product SGN estimation errors.

the experimental product SGN is excellent. The 17 analyzed samples present deviations smaller than 4%; furthermore, 12 of them are within 2% error.

3.2. Variables Sensitivity. Because of its accuracy in predicting the product quality, the granulation circuit model can be considered a suitable tool to represent the operation of granulation urea plants. However, it is important to further evaluate the sensitivity of the most important circuit variables against different key variables that can be manipulated. This sensitivity analysis allows understanding the behavior of the whole circuit and gives insights to design new operating/control strategies.

According to the urea granulation flowsheet shown in Figure 1, the process variables that can be changed during operation are: (a) the urea solution fed to the granulator growth chambers, $\dot{m}_{melt}$ (this variable can be manipulated on line and its value multiplied by the urea concentration of the atomized solution represents the plant capacity), (b) the gap between the rolls of the crusher upper and lower pairs, GAP_U and GAP_L (these variables can be manually adjusted during operation), (c) the top and bottom deck screen apertures, h_T and h_B (which can be changed during plant shutdowns by replacing the decks or can be affected, under normal operation, by clogging or wire deformations that modify the screen passage area), (d) the granulator discharge area, α (which can be varied to control the fluidized bed levels[18,23]), (e) the fluidization air temperature to the growth chambers, T_a (the chamber's temperature can be adjusted by manipulating the steam to the heat exchangers that determine the fluidization air thermal level[21,23]), and (f) the fluidization air flow rate, $\dot{m}_a^T$, that is automatically adjusted to maintain the total pressure drop at a constant value.[16] In fact, $\dot{m}_a^T$ cannot be independently manipulated and depends on the momentum balance (eq A.8; see Appendix) as well as on the established vacuum pressure on the granulator top. For this reason, only the other above-mentioned variables are disturbed in ±10% with respect to the initial steady state to analyze the circuit responses.

The circuit performance under the above different disturbances is studied by monitoring all the operating variables, particularly the screen's oversize (O) and fines (U) mass flow rates, the recycle fraction (defined as the ratio between the material out of specification and the product, $R = (O + U)/P$, where P is product stream mass flow rate), the granulator chamber's temperatures (T_k) and fluidized bed heights (H_k), and the recycle and product stream quality through the corresponding SGNs (SGN_R and SGN_P). The mass fraction of particles within the range 2−4 mm (W_{2-4mm}) in the product stream, which indirectly indicates the population spread in particle size, is also tracked. Because the fluidization air mass flow rate is a function of the chamber's momentum balance, it is additionally monitored.

This study is performed by running different steady-state simulations of the entire granulation circuit in the gPROMS environment. The sensitivity study corresponds to a local sensitivity analysis; in fact, ±10% step changes from the initial value (nominal plant operation) are imposed in the manipulated variables (one by one, i.e., one input factor is changed while the values of other input factors are kept constant), and the circuit performance is studied by monitoring the final steady-state value reached by the selected output variables.

Table 1 shows the operating variables at the final steady state (expressed as percentage of variation with respect to the corresponding initial steady-state values) for the performed disturbances. The shaded values point out the more sensitive circuit variables.

The results clearly indicate that the variables that most influence the circuit performance are the screen's deck apertures. Even though h_T and h_B cannot be modified during normal operation, their variation due to clogging or wire deformation can significantly influence the plant operation. The gap between the lower pair of rolls of the crusher has also a significant effect on the monitored variables, especially on the oversize mass flow rate. Contrarily, variations in the gap between the upper rolls cause minor changes in the main circuit

Table 1. Sensitivity Analysis of the Granulation Circuit Variables

		SGN_P	W_{2-4mm}	R	SGN_R	O	U	T_2	H_2	$\dot{m}_a^T$
GAP_L	10%	1.39	0.46	-4.09	1.25	17.95	-6.11	0.05	-3.78	1.12
	-10%	-1.28	-0.59	4.89	-1.09	15.35	6.74	-0.05	4.20	-1.33
GAP_U	10%	-0.14	-0.04	0.21	-0.22	-1.39	0.36	0.00	0.20	-0.06
	-10%	0.04	0.01	-0.10	0.05	0.45	-0.14	0.00	-0.09	0.03
h_B	10%	1.97	1.23	40.53	5.55	-5.76	44.77	-0.44	18.55	-9.72
	-10%	-2.48	-2.09	-30.94	-7.06	8.83	-34.60	0.57	-16.25	6.04
h_T	10%	6.27	-3.49	-17.30	3.38	-15.37	-17.50	0.24	-14.37	4.28
	-10%	-6.40	-1.98	30.13	-3.32	21.60	30.90	-0.27	21.19	-8.36
$\dot{m}_{melt}$	10%	-0.52	-0.34	-5.84	-1.21	10.55	2.83	1.09	10.04	-4.50
	-10%	0.48	0.30	7.39	1.27	-11.27	-2.63	-1.10	-10.55	4.16
α	10%	0.00	0.00	0.00	0.00	0.01	0.00	-0.25	-10.37	4.07
	-10%	0.00	0.00	0.00	0.00	0.01	0.00	0.36	11.75	-5.63
T_a	10%	0.00	0.00	0.00	0.00	0.01	0.00	1.75	0.20	-0.15
	-10%	0.00	0.00	0.00	0.00	0.01	0.00	-1.76	-0.20	0.15

highly sensitive variables (response greater than ±10% when a ±10% disturbance is assayed)
sensitive variables (response approximately ±10% when a ±10% disturbance is assayed)
moderate sensitive variables (response smaller than ±10% and higher than ±2 %when a ±10% disturbance is assayed)
low sensitive variables (responses smaller than ±2 % when a ±10% disturbance is assayed)

variables. With respect to the urea solution flow rate, it has an important impact on the chamber's heights and the oversize flow rate. Finally, disturbances in the granulator discharge area directly influence the granulator chambers' heights; variations in the fluidization air temperature only slightly influence the chambers' temperatures (i.e., about 1.75%).

The oversize and undersize mass flow rates, together with the recycle ratio and the beds heights, are the most sensitive variables. Particularly, the granulator chambers' heights are considerably affected by disturbances in both screen deck apertures, the urea solution flow rate, and the granulator discharge area. As a consequence, the fluidization air flow rate also changes (see the momentum balance presented in the Appendix, eq A.8). On the other hand, the product and recycle granulometry (i.e., SGN_P, W_{2-4mm}, and SGN_R) are variables defined as less sensitive. Besides, the chambers' temperatures are the most stable monitored variables.

These results enrich the sensitivity analysis performed by Cotabarren et al.[29] because in this contribution, additional manipulated variables are tested (i.e., granulator discharge area and fluidization air temperature) and the fluidized bed granulator model includes the momentum balance between the blower suction and the granulator top. Even though the monitored variables present similar trends under the assayed disturbances (when the granulator momentum balance is or is not considered), it is important to note that the granulator chambers' heights become less sensitive to the variables when the fluidization air flow rate is determined by the granulator momentum balance closure (i.e., the disturbances that increase the fluidized bed levels induce lower air flow rates that partly offset the effect).

3.3. Common Operating Problems. *3.3.1. High Granulator Chambers' Temperatures.* According to practical experience,[18] one of the main issues when operating urea granulation circuits is the too-high levels the chambers' temperatures may reach, particularly the second and third chambers. This is usually associated with either high ambient temperature during the summer season or increments in the plant capacity. As is clear from Table 1, the manipulated variable that most influences the second chamber temperature is the urea solution flow rate; therefore, when the operation policy is to increase plant capacity, the temperature can become an active constraint.

Having too high a temperature in the growth chambers is undesirable because the solid urea particles may become soften and stick together at temperatures close to the urea melting point (i.e., 132 °C). In fact, when particles rapidly agglomerate, the fluidization quality immediately declines and granulator shut down becomes imminent.[15] Because the first chamber receives the seeds stream at a considerably lower temperature (around 70 °C according to Niks et al.[22]), usually the second and third chambers are the ones that have a higher likelihood of surpassing the maximum allowed temperature. Aiming to control the beds' thermal level, the influence of the fluidization air distribution to each chamber on the compartments' temperatures is carefully analyzed in this work.

As is previously mentioned, a single blower takes the atmospheric air that is later derived to each chamber by ducts with regulating dampers (see Figure 2). It is important to note that the present simulator is operated with constant apertures for these dampers, trying to mimic a very common industrial practice (i.e., according to the model presented in the Appendix, the operation is modeled by keeping the parameter K^k_{damper} constant).[25] Therefore, each chamber's air flow rate is defined by the momentum balance; thus, the temperature of each bed cannot be controlled separately. Aiming to make the granulator operation more flexible (i.e. including more degrees of freedom) in this section, the chamber's temperature sensitivity to changes in the dampers apertures is evaluated. These changes are performed indirectly by disturbing the fluidization air flow rate derived to the second and third chambers between ±20%, with an even distribution of the remaining air to the other chambers in order to keep the total fluidization air flow rate constant. Thus, these simulations are performed without considering the granulator momentum balance (see eq A.8 in the Appendix).

Figure 6 presents the temperatures and the fluidized bed heights for the described changes in the fluidization air flow

dx.doi.org/10.1021/ie401650r | Ind. Eng. Chem. Res. 2013, 52, 15198−15210

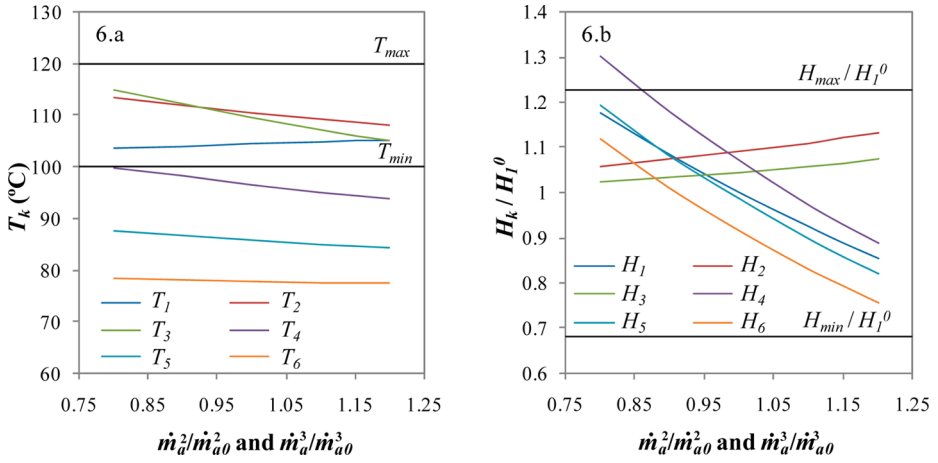

Figure 6. (a) Granulator chambers' temperatures and (b) beds' heights as a function of the magnitude of the disturbance introduced to the fluidization air flow rate derived to the second and third chambers.

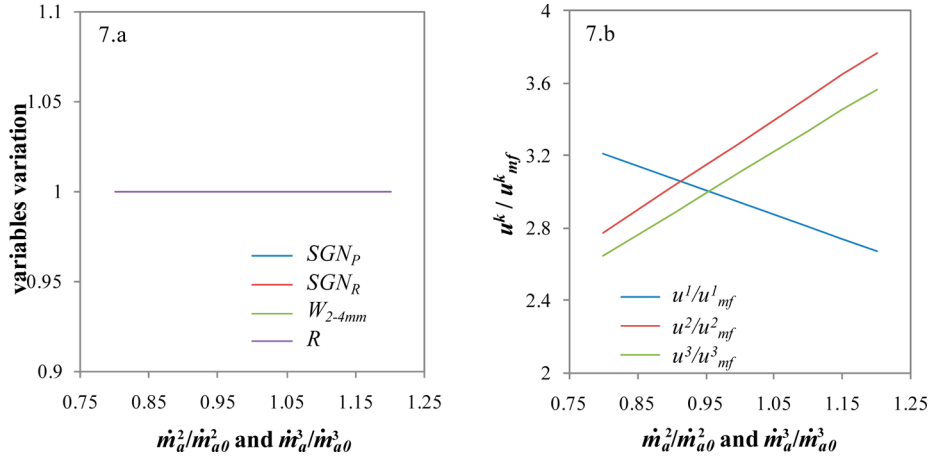

Figure 7. (a) Selected circuit variables and (b) growth chambers' superficial velocity as a function of the magnitude of the disturbance introduced to the fluidization air flow rate derived to the second and third chambers.

rates, the latest referred to the first chamber height value at the base case. As aforementioned, the growth chambers' temperatures and levels need to be within certain ranges to properly operate. In this contribution, it is considered reasonable to operate the growth chambers within 100 and 120 °C and the bed levels between 50% and 80% of the separating weir height (H_{weir}).[23] As expected, when the fluidization air flow rate to the second and third chambers increases, their temperatures decrease. The first chamber temperature increases because its air flow rate decreases, but the opposite is observed in the cooling chambers. This is attributed to the effect of feeding cooler solid streams to these chambers. All the growth chambers' temperatures are within the desired operating range. In fact, using the range 100 °C $\leq T_k \leq$ 120 °C as reference, it is possible to decrease the second and third chambers' temperature 13% and 24%, respectively, when the air flow rates are increased up to 20% with respect to the base case values. Regarding the fluidized bed level, it increases in the second and third compartment with the fluidization air flow rate. Contrarily, it decreases in the first chamber as well as in the cooling ones. The height variations (except H_1 for $\dot{m}_a^2/\dot{m}_{a0}^2$ and $\dot{m}_a^3/\dot{m}_{a0}^3 < 0.88$) are within the operating range, with H_2 and H_3 being the less affected (13% and 7% increments with respect to the initial steady-state, respectively).

It is also interesting to observe the effects of manipulating the dampers' apertures on the streams granulometry and flow rate. Examples of these variables are shown in Figure 7a through the product and recycle stream SGN, the fraction of product on specification, and the recycle ratio. As it can be seen, all the variables remain constant; therefore, changes in the dampers apertures only modify the granulator chambers' temperatures and bed heights. Nonetheless, in order to keep the particles' growth within the coating regime (as discussed in the previous section), special attention has to be paid to the fluidization regime. Numerous authors have demonstrated that changes in the fluidization air flow rate, more specifically in the superficial velocity, can shift the growth regime from coating to agglomeration.[15] As is shown in Figure 7b for chambers 1−3, the superficial velocity (referred to the minimum fluidization velocity) is directly influenced by changes in the fluidization air mass flow rate. However, for the assayed disturbances, the variations in the superficial velocity are relatively low with respect to the base case. It is worth mentioning that for all the tested cases, the superficial velocity corresponding to the Sauter mean size (D_{SV}) is within the minimum fluidization velocity and the elutriation (or terminal) velocity for each chamber's PSD (data not shown).

This analysis demonstrates that it is possible to regulate the chambers' temperatures by manipulating the damper positions.

dx.doi.org/10.1021/ie401650r | Ind. Eng. Chem. Res. 2013, 52, 15198−15210

In fact, this strategy can be useful when determining operating policies to increase plant capacity.[23]

3.3.2. Low Granulator Chambers' Fluidized Bed Heights. According to granular urea production patents, it is highly preferred to spray the urea solution within the fluidized beds (i.e., chambers' fluidized bed levels are higher than the urea solution spray height). In fact, spraying over the bed involves the risk of solidification of the sprayed droplets before they reach any solid seed, clearly promoting dust formation.[21,22] Because of this and the very high sensitivity of the granulator fluidized bed heights against different disturbances (see sensitivity analysis), control of the bed heights becomes extremely important.

The most straightforward way of controlling the chambers' heights involves manipulating the granulator discharge valve (situated at the bottom of the last chamber, according to Figure 2).[23] However, as shown by Cotabarren et al.,[23] the regulation of the fluidized bed levels by closing the granulator discharge also leads to increases in the chambers' temperatures (unwanted effect). Nonetheless, and as is discussed in the previous section, the fluidization air flow rate has also an important and direct effect on the fluidized bed heights. Even though the fluidization air changes also modify the beds' temperature, its capacity to regulate the chambers' heights can be explored.

Under normal operation, the fluidization air flow rate is determined by the momentum balance presented in eq A.8. By carefully examining this equation, it can be seen that a different total air flow rate can be achieved if a different granulator top vacuum pressure, P_{top}, is set (see Figure 2). In other words and by means of the developed flowsheeting tool, changes in the total granulator pressure drop are tested in order to evaluate an alternative to adjust the granulator chambers' levels.

Figure 8 shows that the fluidization air flow rate evolves quite proportionally to changes in the system pressure drop given by

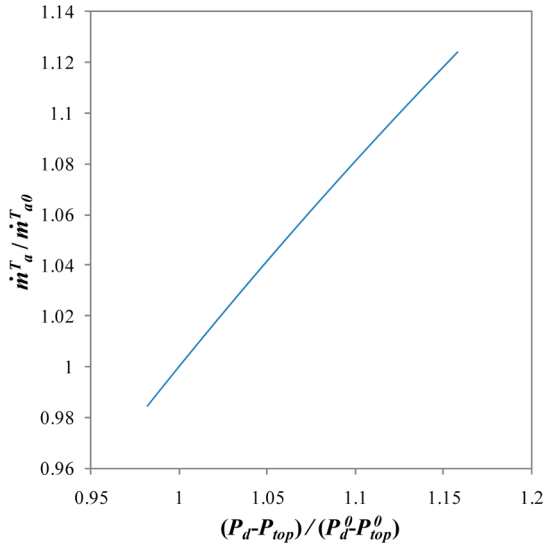

Figure 8. Dimensionless fluidization air flow rate changes as a function of the ratio between the actual system pressure drop and the system pressure drop of the base case.

$P_d - P_{top}$, where P_d is the blower discharge pressure (given by the manufacturer's performance curve evaluated at the corresponding $\dot{m}_a^T$).

In accordance with this result, Figure 9 shows that the granulator fluidized bed heights increase (Figure 9a) and the chambers' temperatures decrease (Figure 9b) as the system pressure drop is increased. In fact, the bed heights for the second, third, and fourth chambers reach and even surpass the maximum allowable level. All the chambers' heights increase approximately 20% when the fluidization air flow rate increases 12% with respect to the initial steady state. The increment in the fluidization air flow rate is accompanied, as expected, by decreases in the chambers' temperatures, all within the desired ranges.

For the maximum tested air flow rate and when the allowable temperature range as reference is considered, it is possible to decrease by 14% and 19% the second and third chambers' temperatures, respectively. Regarding the streams granulometry and mass flow rate, no effect is observed when manipulating the granulator top vacuum pressure (data not shown).

The regulation of the granulator top vacuum pressure (by manipulation of the downstream exhaust fans) can be an overwhelming strategy to control the fluidized bed levels, maintaining the temperatures within the optimum operating range.

3.3.3. Undesired Dust Levels. According to industrial practice, many operating problems are associated with undesired dust levels. The formation of lumps within the granulator or of deposits on the unit walls and air distributor, which can eventually lead to plant shutdowns, are usually attributed to dust generation.[18] Additionally, circulating dust can cause the formation of deposits on the screen decks that affect the separation efficiency giving low product quality and even important changes in the granulator variables (e.g., bed heights). The high dust levels also strongly affect the treatment of the granulator exhaust air which may be overloaded with very fine urea particles.[18,21]

Different factors during plant operation can produce undesired increases in the dust circulating through the circuit. The water content of the urea solution fed to the granulator is a parameter that needs to be carefully monitored. Indeed, increments in the solution water content increase the dust levels.[18,21,22] Furthermore, and as previously mentioned, the urea solution bed overspray clearly promotes dust formation.[21,22] Atomization pressure is a parameter that directly affects the droplet size and also needs to be cautiously tracked to keep dust generation under control; the higher the atomization pressure, the smaller the sprayed droplets.[21,22] Regarding the peripheral units, the crushers' operation should be properly controlled to avoid very fine broken product. Certainly, too much dust in the granulation unit can cause agglomeration or lead to high entrainment flow rates.[18,21]

In this work, the developed simulator is used to test the viability of other flowsheet configurations, alternatives to the one presented in Figure 1, to control the fines level within the circuit. The likelihood of incorporating a screen at the crusher outlet to separate the finer particles is particularly explored. This alternative contemplates the separation of a specified amount of particles smaller than a certain size, which is subsequently reprocessed and injected in the granulation unit as urea solution (i.e., plant capacity remains constant). The corresponding new flowsheet is schematized in Figure 10.

Different bypass alternatives are studied, including the total or partial separation of (a) particles smaller than 1 mm, (b) particles smaller than 2 mm, and (c) the stream without being classified by size. In real practice, the first two options implicate

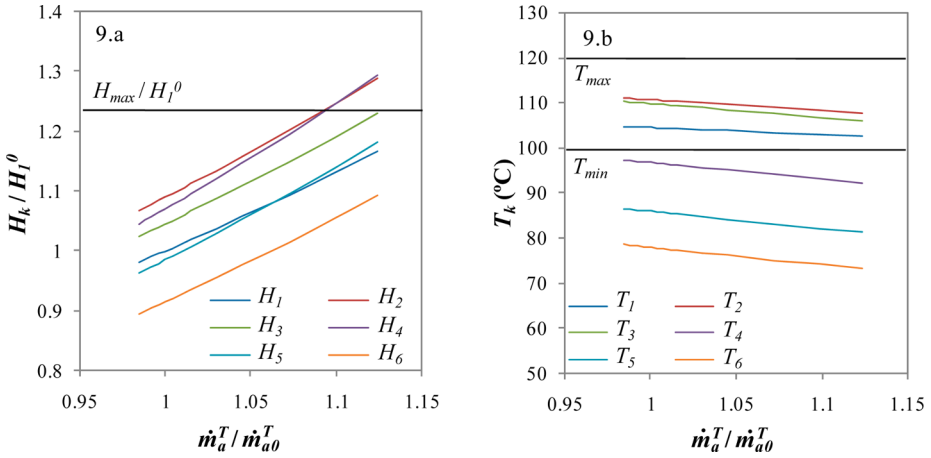

Figure 9. (a) Dimensionless granulator chamber heights and (b) chamber temperatures for variations in the total fluidization air flow rate originated by changes in the granulator top vacuum pressure.

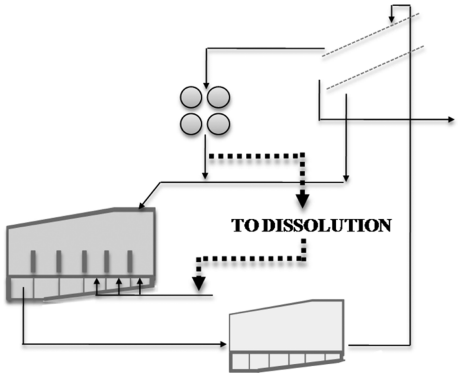

Figure 10. Alternative granulation circuit flowsheet.

the addition of a screen with deck openings according to the desired size and different separation efficiency and the last one implies the partial or total derivation of the stream.

The final steady-state values of the selected product stream's variables found through simulations carried out under different bypass fractions (*BF*) for cases a, b, and c are presented in Figure 11. As can be seen, the derivation and reuse of particles smaller than 1 mm allows increasing the fraction of product on specification for the whole range of bypass fractions. The bypass of particles smaller than 2 mm and of the stream with no size classification gives a maximum value for W_{2-4mm} at *BF* = 0.8 and *BF* = 0.7, respectively (Figure 11a). As expected, the SGN_P increases as fines are removed from the circuit. Moreover, and for certain bypass fractions, SGN_P exceeds the maximum value established by the international trade standards.[30,31]

Regarding the granulation unit, Figure 12 presents the different steady states reached by the second chamber temperature and the last chamber height for the alternatives a, b, and c. The increment in the urea solution injected to each chamber (associated to the bypass) is reflected in higher chamber temperatures. For bypass fractions greater than 0.8 of the stream with no size classification, the second chamber temperature exceeds the maximum allowable value.[21] The same occurs when more than 95% of the particles smaller than 2 mm are bypassed. On the other hand, the second chamber temperature is lower than its maximum limit even for the total bypass of particles smaller than 1 mm (Figure 12a). The chambers' heights present different behaviors according to the fraction and size of bypassed material. For the bypass of particles smaller than 1 mm, the fluidized bed levels decrease monotonically with the bypass fraction because the mass flow rate recycled to the granulator is small. Actually, the last chamber height reaches its minimum allowable value when the 100% of particles smaller than 1 mm are bypassed. The

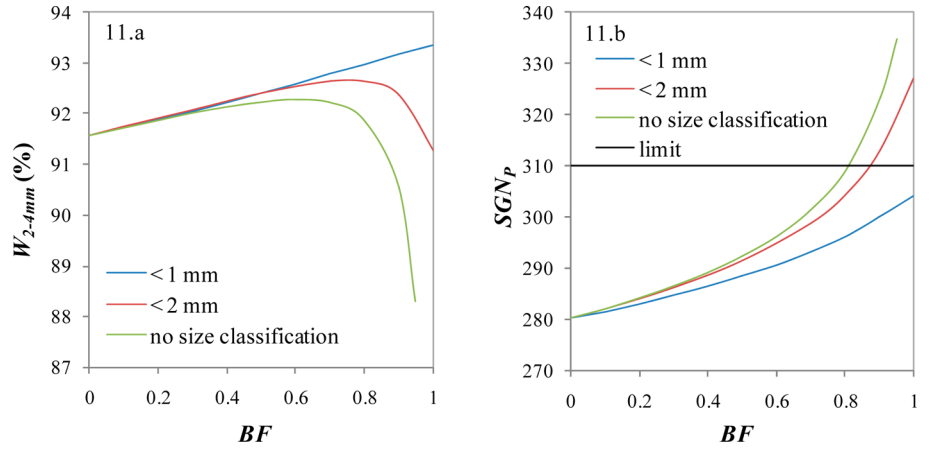

Figure 11. Product stream variables for different bypass fractions of the crusher outlet stream.

dx.doi.org/10.1021/ie401650r | *Ind. Eng. Chem. Res.* 2013, 52, 15198−15210

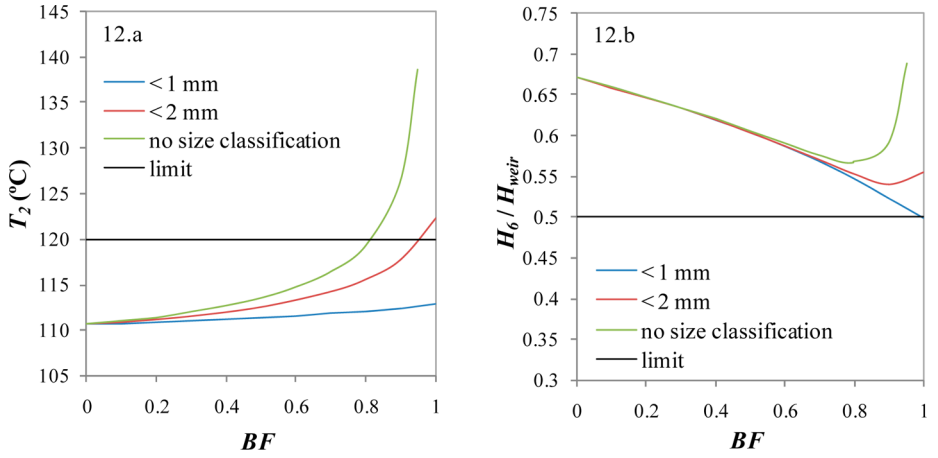

Figure 12. Granulator variables for different bypass fractions of the crusher outlet stream.

decreasing height behavior is also observed for low bypass fractions of the other two cases (particles smaller than 2 mm and the stream with no size classification). However, as soon as the increment in the flow rate of injected urea solution becomes more significant than the decrease in the seeds flow rate, the fluidized bed levels start to increase (Figure 12b).

From all the tested options, it seems promising to reduce the fines circulating through the circuit by bypassing as much material as possible of the particles smaller than 1 mm. In fact, a lower risk of agglomeration is expected with this alternative flowsheet. Furthermore, the performed simulations indicate that the fraction of product on specification increases, maintaining the other key circuit variables within the allowable operating ranges.

It is important to note that as the bypass fraction of the stream without classification tends to 1, the monitored variables become significantly affected. Certainly, for *BF* very close to 1, the simulator presents convergence issues. This clearly demonstrates the function of the crusher as a generator of nuclei for the granulation unit. Besides, previous authors have shown that the granulation circuit becomes less stable as the flow rate of the crushed material diminishes.[8,11,32−34]

The evaluation of alternative flowsheets to tackle traditional high dust level problems is a novel strategy that has not been previously explored. Moreover, a new set of studies can be carried out with this new configuration to not only acknowledge the circuit sensitivity to traditional manipulated variables but also to perform optimizations or propose process control strategies.

4. CONCLUSIONS

For a large-scale industrial granulation circuit, a flowsheeting tool (based on previous contributions and improved by taking into account the momentum balance in the granulator unit) has been validated and used to analyze the effect of different operation policies on the plant performance.

Good correspondence between experimental and simulated data is obtained by using the developed granulator circuit simulator; particularly, the product stream main properties are well-predicted. Because only the crusher and screen units' models were previously and separately validated, this constitutes a valuable result. In effect, this implies that the granulator and cooler models, which do not involve fitted parameters, represent quite precisely the real operation. Moreover, this indicates that the recycle stream is properly solved and its mass flow rate, PSD, and temperature are well predicted.

The presented local sensitivity analysis gives good insights to optimize the operation of granulation circuits. In fact, a new way of controlling the quite insensitive chambers' temperatures is explored by manipulating the fluidization air dampers. It is demonstrated that good control of the undesired high growth chambers' temperatures can be achieved, maintaining the fluidized bed heights within the desired operating range.

The performed simulations also show that it is possible to regulate the fluidized bed heights by changing the granulator top vacuum pressure, which indirectly modifies the total fluidization air flow rate. This alternative result is attractive when the objective is to avoid low fluidized bed levels because, contrary to the manipulation of the granulator discharge, this action diminishes the growth chambers' temperatures.

Finally, and for reducing dust formation, an alternative flowsheet configuration that consists in partially bypassing the fines that leave the crusher unit is proposed and tested. The bypass of particles smaller than 1 mm proves to be an efficient alternative for reducing the circulating dust and incrementing the fraction of product on specification, maintaining all the circuit variables within the operating range.

■ APPENDIX

This appendix briefly presents the equations of the fluidized bed granulator model described in Section 2, based on Bertin et al.[24] and Cotabarren et al.[25] The dynamic urea mass balance for chamber k is

$$\frac{dm_T^k}{dt} = \dot{m}_{in}^k + \dot{m}_{melt}^k(1 - x_{melt}^k) - \dot{m}_{out}^k \qquad m_T^k(0) = m_{T0}^k \tag{A.1}$$

where t represents the time, m_T^k, $\dot{m}_{in}^k$, and $\dot{m}_{out}^k$ are the solid mass holdup and inlet and outlet particles mass flow rates, respectively, and $\dot{m}_{melt}^k$ and x_{melt}^k are the urea solution mass flow rate atomized into chamber k and its water mass fraction, respectively. According to Bertin et al.,[20] it is accurate to assume that the urea solution's water content evaporates immediately and completely; therefore, the water mass balance can be neglected. The outlet solids mass flow rates are obtained by applying the Bernoulli equation

dx.doi.org/10.1021/ie401650r | Ind. Eng. Chem. Res. 2013, 52, 15198−15210

$$\dot{m}_{\text{out}}^{k} = C_D A_o^{k} \sqrt{2g\rho_{\text{bed}}^{k}(\rho_{\text{bed}}^{k} H_k - \rho_{\text{bed}}^{k+1} H_{k+1})} \qquad k = 1{-}5 \tag{A.2}$$

$$\dot{m}_{\text{out}}^{6} = C_D A_o^{6} \rho_{\text{bed}}^{6} \sqrt{2gH_6} \tag{A.3}$$

where A_0^k and H_k are the passage area and fluidized bed height of chamber k, respectively. C_D is the discharge coefficient and ρ_{bed}^k is the bed density in compartment k as given by Bertin et al.[24]

To complete the set of equations, the fluidized bed height within each chamber is computed as:

$$H_k = \frac{m_T^k}{\rho_{\text{bed}}^k A_T^k} \tag{A.4}$$

being A_T^k the cross-sectional area of chamber k.

The following dynamic energy balance given by Bertin et al.[24] is considered to compute the temperature T_k in each chamber:

$$\begin{aligned} m_T^k Cp_u(T_k)\frac{dT_k}{dt} &= \dot{m}_{\text{in}}^k \int_{T_k}^{T_{k-1}} Cp_u\, dT \\ &+ \dot{m}_{\text{melt}}^k(1 - x_{\text{melt}}^k) \int_{T_k}^{T_{\text{melt}}^k} Cp_u\, dT \\ &+ \dot{m}_{\text{melt}}^k x_{\text{melt}}^k \int_{T_k}^{T_{\text{melt}}^k} Cp_w\, dT - \dot{m}_{\text{melt}}^k x_{\text{melt}}^k \Delta H_{EV}(T_k) \\ &+ \dot{m}_{\text{melt}}^k(1 - x_{\text{melt}}^k)\Delta H_{DIS}(T_{\text{melt}}^k) + \dot{m}_a^k \int_{T_k}^{T_a^k} Cp_a\, dT \\ &+ \dot{m}_a^k Y_{a_{in}}^k \int_{T_k}^{T_a^k} Cp_v\, dT \qquad T_k(0) = T_0^k \end{aligned} \tag{A.5}$$

where T_{melt}^k, T_a^k and T_{k-1} are the temperatures of the melt, fluidization air, and solids entering chamber k, respectively. T_k is the chamber temperature and, according to previous studies, can be accurately considered equal to the solid and air outlet temperatures.[20] For the granulator first chamber, $T_{k\text{-}1}$ and $\dot{m}_{\text{in}}^k$ correspond to the seed temperature and mass flow rate, respectively. ΔH_{DIS} and ΔH_{EV} are the latent heats associated to the urea melt dissolution and water evaporation. Cp_u, Cp_w, Cp_a, and Cp_v are the mass heat capacities of the solid urea, liquid water, air, and water vapor, respectively. It is worth mentioning that according to one of the model hypothesis, the gaseous and liquid phases operate at pseudosteady state. Thus, the mass and energy accumulations of air and liquid within the fluidized chambers are neglected.[20] The energy balance complete derivation can be found elsewhere.[7]

Bertin et al.[24] developed a population balance model for the urea fluidized bed granulator assuming that only growth by coating occurs (elutriation, agglomeration, breakage, attrition, and nucleation were assumed negligible). Thus, the dynamic population balance equation (PBE) for each well-mixed granulation chamber is given by

$$\frac{\partial n^k}{\partial t} + \frac{\partial(G_k n^k)}{\partial d} = \dot{n}_{\text{in}}^k - \dot{n}_{\text{out}}^k \qquad \text{IC: } n^k(d, 0) = n_0^k(d)$$
$$\text{BC: } n^k(0, t) = 0 \tag{A.6}$$

where G_k is the growth rate, d the particles diameter, $\dot{n}_{\text{in}}^k$and $\dot{n}_{\text{out}}^k$ the number density function flows in and out of chamber k, and $n_0^k(d)$ the number density function at the initial time, respectively. The PBE discretization technique developed by Hounslow et al.[35] and adopted by Bertin et al.[24] is implemented to solve the discretized form of eq A.6.

Assuming that particles belonging to different size intervals grow proportional to its fractional surface area, G_k is defined as

$$G_k = \frac{2\dot{m}_{\text{melt}}^k(1 - x_{\text{melt}}^k)}{\rho_p A p_T^k} \tag{A.7}$$

where Ap_T^k denotes the total particles surface area within chamber k and ρ_P the particles density. This equation states that all the particles, independent of their sizes, grow at the same rate.[9,16,24]

Finally, the momentum balance between the blower suction and the granulator top (which has not been considered in the models previously published) can be written as[25]

$$\begin{aligned} &-\frac{0.5}{\rho_a^{\text{in}}}\left(\frac{\dot{m}_a^T}{A_T^{\text{blower}}}\right)^2 + \rho_a^k g H_k + (P_{\text{top}} - P_{\text{atm}}) - \Delta P_{\text{blower}} \\ &+ K_{\text{damper}}^k \frac{\dot{m}_a^{k^2}}{\rho_{ak}^{\text{damper}}} + \frac{K_{\text{grid}}}{\rho_{ak}^{\text{grid}}}\left(\frac{\dot{m}_a^k}{A_T^k}\right)^2 + (\rho_p - \rho_a^k) g(1 - \varepsilon^k) \\ &H_k = 0 \qquad k = 1{-}6 \end{aligned} \tag{A.8}$$

The first term corresponds to the change in the kinetic energy between the blower suction and the granulator top, with ρ_a^{in} and A_T^{blower} being the fluidization air density and the duct cross-sectional area at the blower suction, respectively; $\dot{m}_a^T$ represents the total fluidization air flow rate (i.e., the sum of every chamber fluidization air flow rate, $\dot{m}_a^k$). As the granulator top cross-sectional area is considerably bigger than that of the blower suction duct, the air velocity at this point can be neglected. The second term represents the change in the potential energy, which only takes into account the contribution of the fluidized bed height (H_k). Regarding the third term, atmospheric conditions are assumed at the blower suction, and the top granulator pressure is set at the desired vacuum value (by means of downstream exhaust fans) to guarantee proper dust suction.[19] ΔP_{blower} (i.e., $P_d - P_{\text{atm}}$, with P_d as the blower discharge pressure) represents the energy supplied by the blower (that is determined through the manufacturer's performance curve) and depends on $\dot{m}_a^T$. The following term corresponds to the friction losses generated by the dampers; these are usually set at constant aperture, being the corresponding friction losses a function of the respective air mass flow rates, the air density at the damper ($\rho_{ak}^{\text{damper}}$) and a constant parameter that depends on the damper aperture (K_{damper}^k). The sixth term is related with the friction losses in the perforated plate (i.e., grid) and is proportional to the square velocity of the air that passes through it. K_{grid} is a constant that depends on the design and geometry of the perforated plate.[16] For chamber k, A_T^k represents the cross-sectional area and ρ_{ak}^{grid} the air density at the grid entrance. The last term accounts for the friction pressure drop in each fluidized bed, which is a result of the force balance between the particles and the fluid,[16,36] where ρ_a^k is the air density and ε^k the porosity corresponding to chamber k. The values for the damper (K_{damper}^k) and grid (K_{grid}) constants can be found elsewhere.[25]

List of Symbols

A_0^k = Passage area for granulator chamber k [m^2]
Ap_T^k = Total particles superficial area for granulator chamber k [m^2]

dx.doi.org/10.1021/ie401650r | Ind. Eng. Chem. Res. 2013, 52, 15198−15210

A_T^{blower} = Blower duct cross-sectional area [m^2]
A_T^k = Cross-sectional area for granulator chamber k [m^2]
BF = Bypass fraction [-]
C_D = Discharge coefficient [-]
Cp_a = Air mass heat capacity [J/(kg °C)]
Cp_u = Solid urea mass heat capacity [J/(kg °C)]
Cp_v = Water vapor mass heat capacity [J/(kg °C)]
Cp_w = Liquid water mass heat capacity [J/(kg °C)]
d = Particles diameter [m]
D_{SV} = Sauter mean size [m]
g = Gravity acceleration [m/s^2]
G_k = Growth rate for granulator chamber k [m/s]
GAP_U = Distance between the crusher upper pair of rolls [m]
GAP_L = Distance between the crusher lower pair of rolls [m]
h_B = Screen bottom deck aperture [m]
H_1^0 = First chamber height at the initial steady state [m]
H_k = Fluidized bed height for granulator chamber k [m]
H_{max} = Maximum allowable operating fluidized bed height [m]
H_{min} = Minimum allowable operating fluidized bed height [m]
h_T = Screen top deck aperture [m]
H_{weir} = Separating weir height [m]
K_{damper}^k = Damper constant parameter for granulator chamber k [-]
K_{grid} = Grid constant parameter [-]
$\dot{m}_a^k$ = Fluidization air mass flow rate for granulator chamber k [kg/s]
$\dot{m}_a^T$ = Total fluidization air mass flow rate [kg/s]
$\dot{m}_{a0}^T$ = Total fluidization air mass flow rate at the initial steady state [kg/s]
$\bar{m}_i^{ap}$ = Mass fraction for class i particles expressed as a normalized cumulative function [-]
$\dot{m}_{in}^k$ = Inlet mass flow rate for granulator chamber k [kg/s]
$\dot{m}_{melt}^k$ = Urea solution mass flow rate for granulator chamber k [kg/s]
$\dot{m}_{out}^k$ = Outlet mass flow rate for granulator chamber k [kg/s]
m_T^k = Mass holdup for granulator chamber k [kg]
m_{T0}^k = Mass holdup for granulator chamber k at the initial steady state [kg]
n^k = Number density function for granulator chamber k [#/m]
n_0^k = Number density function for granulator chamber k at the initial steady state [#/m]
$\dot{n}_{in}^k$ = Inlet number flow rate expressed as density function for granulator chamber k [#/m s]
$\dot{n}_{out}^k$ = Outlet number flow rate expressed as density function for granulator chamber k [#/m s]
O = Oversize stream mass flow rate [kg/s]
P = Product stream mass flow rate [kg/s]
P_{atm} = Atmospheric pressure [Pa]
P_d = Blower discharge pressure [Pa]
P_d^0 = Blower discharge pressure at the initial steady state [Pa]
P_{top} = Granulator top vacuum pressure [Pa]
P_{top}^0 = Granulator top vacuum pressure at the initial steady state [Pa]
R = Recycle fraction [-]
SGN_P = Product stream size guide number [mm × 100]
SGN_R = Recycle stream size guide number [mm × 100]
T_a^k = Fluidization air temperature for chamber k [°C]
T_k = Temperature for granulator chamber k [°C]
T_0^k = Temperature for granulator chamber k at the initial steady state [°C]
T_{max} = Maximum allowable operating temperature [°C]
T_{min} = Minimum allowable operating temperature [°C]
T_{melt}^k = Urea solution temperature for granulator chamber k [°C]
U = Undersize stream mass flow rate [kg/s]
u^k = Air superficial velocity for granulator chamber k [m/s]
u_{mf}^k = Minimum fluidization air velocity for granulator chamber k [m/s]
W_{2-4mm} = Mass fraction between 2 and 4 mm in the product stream [-]
x_{melt}^k = Urea solution water mass fraction for granulator chamber k [-]
$Y_{a_{in}}^k$ = Mass inlet air humidity for granulator chamber k, dry basis [-]

Greek Symbols

α	Fraction of the granulator discharge area [-]
ΔH_{DIS}	Urea melt dissolution latent heat [J/kg]
ΔH_{EV}	Water evaporation latent heat [J/kg]
ΔP_{blower}	Energy supplied by the air blower [Pa]
ε^k	fluidized bed porosity for granulator chamber k [-]
ρ_a^k	Air density for granulator chamber k [kg/m^3]
$\rho_{a,k}^{damper}$	Fluidization air density in the damper for granulator chamber k [kg/m^3]
$\rho_{a,k}^{grid}$	Fluidization air density in the grid for granulator chamber k [kg/m^3]
ρ_a^{in}	Fluidization air density in the blower suction [kg/m^3]
ρ_{bed}^k	fluidized bed density for granulator chamber k [kg/m^3]
ρ_P	Urea particles density [kg/m^3]

AUTHOR INFORMATION

Corresponding Author

*I. M. Cotabarren. Phone: 54-291-486-1700, ext 269. Fax: 54-291-486-1600. E-mail: icotabarren@plapiqui.edu.ar.

Notes

The authors declare no competing financial interest.

ACKNOWLEDGMENTS

The authors express their gratitude for the financial support by the Consejo Nacional de Investigaciones Científicas y Técnicas (CONICET), Agencia Nacional de Promoción Científica y Tecnológica (ANPCyT), and Universidad Nacional del Sur (UNS) of Argentina.

REFERENCES

(1) Aspen Technology Inc. http://www.aspentech.com (accessed Oct 10, 2013).
(2) *gPROMS*. Process System Enterprise. http://www.psenterprise.com (accessed Oct 10, 2013).
(3) *Pro/II*. Invensys Operation Management. http://iom.invensys.com (accessed Oct 10, 2013).
(4) Reimers, C.; Werther, J.; Gruhn, G. Design specifications in the flowsheet simulation of complex solids processes. *Powder Technol.* **2009**, *191*, 260−271.
(5) Werther, J.; Heinrich, S.; Dosta, M.; Hartge, E.-U. The ultimate goal of modeling—Simulation of system and plant performance. *Particuology* **2011**, *9*, 320−329.
(6) Schwier, D.; Hartge, E.-U.; Werther, J.; Gruhn, G. Global sensitivity analysis in the flowsheet simulation of solids processes. *Chem. Eng. Process.* **2010**, *49*, 9−21.
(7) Cotabarren, I. M. *Modelado y Simulación del Sector de Granulación de una Planta de Urea*; Universidad Nacional del Sur: Buenos Aires, Argentina, 2012.
(8) Drechsler, J.; Peglow, M.; Heinrich, S.; Ihlow, M.; Morl, L. Investigating the dynamic behaviour of fluidized bed spray granulation

processes applying numerical simulation tools. *Chem. Eng. Sci.* **2005**, *60*, 3817−3833.
(9) Litster, J. D.; Ennis, B. J.; Liu, L. *The Science and Engineering of Granulation Processes*; Particle Technology Series, Kluwer Academic Publishers: Dordrecht, The Netherlands, 2004.
(10) Cameron, I. T.; Wang, F. Y.; Immanuel, C. D.; Stepánek, F. Process systems modelling and applications in granulation: A review. *Chem. Eng. Sci.* **2005**, *60*, 3723−3750.
(11) Dosta, M.; Heinrich, S.; Werther, J. Fluidized bed spray granulation: Analysis of the system behaviour by means of dynamic flowsheet simulation. *Powder Technol.* **2010**, *204*, 71−82.
(12) Reimers, C.; Werther, J.; Gruhn, G. Flowsheet simulation of solids processes. Data reconciliation and adjustment of model parameters. *Chem. Eng. Process.* **2008**, *47*, 138−158.
(13) Dosta, M.; Antonyuk, S.; Heinrich, S. Multiscale simulation of the fluidized bed granulation process. *Chem. Eng. Technol.* **2012**, *35*, 1373−1380.
(14) Heffer, P.; Prud'homme, M. Fertilizer Outlook 2012−2016. In *Int. Fert. Ind. Assoc. Annu. Conf., 80th*; International Fertilizer Industry Association: Paris, 2012.
(15) Cotabarren, I. M.; Bertín, D. E.; Veliz, S.; Mirazú, L.; Piña, J.; Bucalá, V. Production of Granular Urea as Nitrogenous Fertilizer. In *Urea: Synthesis, Properties and Uses*; Muñoz, C. M.; Fernández, A. M., Eds.; NOVA Publishers: Hauppauge, New York, 2012; pp 1−63.
(16) Mörl, L.; Heinrich, S.; Peglow, M. Fluidized Bed Spray Granulation. In *Handbook of Powder Technology*; Salman, A. D.; Hounslow, M. J.; Seville, J. P. K., Eds.; Elsevier: Amsterdam, The Netherlands, 2007.
(17) Cotabarren, I. M.; Schulz, P. G.; Bucalá, V.; Piña, J. Modeling of an industrial double-roll crusher of a urea granulation circuit. *Powder Technol.* **2008**, *183*, 224−230.
(18) Alnajar, A. Framing the best practices in granulation operation. *Arab Fertilizer* **2010**, *58*, 26−29.
(19) Kayaert, A. N.S.M. fluidised-bed urea granulation process. *Proc. Annu. Meet.—Fert. Ind. Round Table, 30th*; Fertilizer Industry Round Table: Baltimore, MD, 1980.
(20) Bertín, D. E.; Mazza, G.; Piña, J.; Bucalá, V. Modeling of an industrial fluidized bed granulator for urea production. *Ind. Eng. Chem. Res.* **2007**, *46*, 7667−7676.
(21) Kayaert, A.; Antonus, R. Process for the production of urea granules. U.S. Patent 5,653,781. 1997.
(22) Niks, A.; Van Hijfte, W.; Goethals, R. Process for urea granulation. U.S. Patent 4,219,589. 1980.
(23) Cotabarren, I. M.; Bertín, D. E.; Piña, J.; Bucalá, V. Analysis of optimal control problems and plant debottlenecking for urea granulation circuits. *Ind. Eng. Chem. Res.* **2011**, *50*, 11996−12010.
(24) Bertín, D. E.; Cotabarren, I. M.; Bucalá, V.; Piña, J. Analysis of the product granulometry, temperature and mass flow of an industrial multichamber fluidized bed urea granulator. *Powder Technol.* **2011**, *206*, 122−131.
(25) Cotabarren, I. M.; Bertín, D. E.; Bucalá, V.; Piña, J. Dynamic optimization of a urea granulation circuit. *Int. Granulation Workshop, 5th*; The University of Sheffield: Sheffield, U. K., 2011.
(26) Cotabarren, I. M.; Rossit, J.; Bucalá, V.; Piña, J. Modeling of an industrial vibrating double-deck screen of a urea granulation circuit. *Ind. Eng. Chem. Res.* **2009**, *48*, 3187−3196.
(27) *gPROMS Documentation*, Release 3.2.0; Process Systems Enterprise: London, 2009.
(28) Nowee, S. M.; Abbas, A.; Romagnoli, J. Model-based optimal strategies for controlling particle size in antisolvent crystallization operations. *Cryst. Growth Des.* **2008**, *8*, 2698−2706.
(29) Cotabarren, I. M.; Bertín, D.; Bucalá, V.; Romagnoli, J.; Piña, J. Dynamic simulation and optimization of a urea granulation circuit. *Ind. Eng. Chem. Res.* **2010**, *49* (14), 6630−6640.
(30) CF Industries: Deerfield, IL. http://cfindustries.com/producturea.htm (accessed Oct 10, 2013).
(31) Karnaphuli Fertilizer Co. Ltd.: Rangadia, Anowara Chittagong, Bangladesh. http://www.kafcobd.com/html/products.html (accessed Oct 10, 2013).
(32) Heinrich, S.; Peglow, M.; Ihlow, M.; Henneberg, M.; Morl, L. Analysis of the start-up process in continuous fluidized bed spray granulation by population balance modelling. *Chem. Eng. Sci.* **2002**, *57*, 4369−4390.
(33) Heinrich, S.; Peglow, M.; Ihlow, M.; Morl, L. Particle population modeling in fluidized bed-spray granulation—analysis of the steady state and unsteady behavior. *Powder Technol.* **2003**, *130*, 154−161.
(34) Radichkov, R.; Muller, T.; Kienle, A.; Heinrich, S.; Peglow, M.; Morl, L. A numerical bifurcation analysis of continuous fluidized bed spray granulation with external product classification. *Chem. Eng. Process.* **2006**, *45*, 826−837.
(35) Hounslow, M. J.; Ryall, R.; Marshall, V. R. A discretized population balance for nucleation, growth, and aggregation. *AIChE J.* **1988**, *34*, 1821−1832.
(36) Kunii, D.; Levenspiel, O. *Fluidization Engineering*; Butterworth-Heinemann: Newton, MA, 1991.